UNIVERSITY OF TWENTE.

Faculty of Electrical Engineering,
Mathematics & Computer Science

Modeling Receiver Properties to Quantify The Receiver performance

Mayuranjanie Sivaraj
M.Sc. Thesis
August 2016

Supervisors:

Dr. ir. M.J.Bentum
Prof. Dr. ir. Ing. F.B.J.C.Leferink
Dr. ing. E.A.M.Klumperink
Van de Beek, G.S., M.Sc.

Telecommunication Engineering Group
Faculty of Electrical Engineering,
Mathematics and Computer Science
University of Twente
P.O. Box 217

Summary

The receiver performance can be limited due to a number of reasons. Desensitization is one of the key issues that degrades the overall performance of the receiver. Desensitization is caused, when strong interferers at the receiver input leading to nonlinear behavior of the receiver front end. Under such conditions, the receiver experiences gain compression, increase in overall noise figure, and distortion products affecting the desired signal, which in turn produces decreased signal to noise ratio (SNR) at the input of the demodulator.

For this purpose, behavioral modeling based on empirical measurements on low noise amplifier (LNA) when exposed to out of band blockers (OOB) was developed with a help of MATLAB to investigate the nonlinear behavior and quantify the receiver performance in terms of error vector magnitude (EVM). The model was verified with measurement results. Additionally, EVM was used to predict the SNR of the receiver system and BER performance for different digital modulation schemes under blocker conditions were generated.

List of Abbreviations

AWGN	Additive white Gaussian noise
BER	Bit error rate
BPF	Bandpass filter
BPSK	Binary phase shift keying
BRF	Band reject filter
CW	Continuous wave
DUT	Device under test
Eb/No	Signal to noise ratio per bit
EVM	Error vector magnitude
IF	Intermediate frequency
IIP3	Input third order intercept point
LNA	Low noise amplifier
LO	Local oscillator
MDS	Minimum detectable signal
OOB	Out of band blocker
QAM	Quadrature amplitude modulation
QPSK	Quadrature phase shift keying
RF	Radio frequency
RMS	Root mean square
SFDR	Spurious free dynamic range
SNR	Signal to noise ratio
VSA	Vector signal analyzer
VSG	Vector signal generator

Table of Contents

Chapter 1

1. Introduction

Wireless devices have found applications in wide range of fields. The proliferation of these devices in the recent past has led to crowding of wireless spectrum and thus leading to stringent demands for receiver design. One of the major issues that concern the receiver design is interference mitigation. Since wireless communication systems are susceptible to interference, it’s important to understand the effects of interference on receivers. Electromagnetic interference can be classified into two broad categories,

- Intentional interference/Intelligent jamming
- Unintentional interference

Intentional interference is usually manmade and unintentional interference can arise from adjacent transmitters emitting frequencies that fall under passband of the receivers or coupling from other electronic devices. These interference have following effects on receivers [1].

1. Physical damage: Causing permanent damage to the receiver
2. Desensitization: Saturating the receiver leading to nonlinear performance
3. Masking: Receiver unable to detect the wanted signal

This project will focus on measurement based modeling of receiver desensitization effects (blocker noise figure, and gain compression) on low noise amplifier (LNA). Since some of the wireless receivers do not include surface wave acoustic (SAW) filters in front of LNA to reject the out of band (OOB) interferers. This is because the practical implementation of such filters on chip is not possible [16]. In such cases, the RF front becomes vulnerable to strong interferers falling in the passband of the receiver. For this purpose, model based empirical measurements on nonlinear device is performed to quantify the effects of receiver desensitization.

1.1 Research Motivation

The main objective of this project is to model the nonlinear properties of the RF front end under blocker conditions to predict the loss of performance the receiver. This involves modeling blocker noise figure and gain compression in the presence of a strong interferer.

Research Question

How do blocker noise figure and gain compression effect the performance of the receiver?

How well the proposed model does fit the measurement?

1.2 Overview

The remaining part of the thesis is organized into four chapters. Chapter 2 presents relevant theory needed for behavioral modeling of nonlinear effects of receiver front end when exposed to large interferers. Chapter 3 presents the experimental setup for two tone measurement, and blocker noise figure measurement of the DUT. In Chapter 4, the measurement and the simulation results were discussed. Finally, in Chapter 5, conclusions of this thesis work and recommendations for future work are presented.

Chapter 2

2. Behavioral Modeling of Receiver Front end

As an aid to the previous chapter, this chapter presents the reader with the required theory behind the nonlinearities associated with RF front end, behavioral modeling of blocker noise figure and gain compression of LNA, and modeling of the entire receiver system. Further, error vector magnitude (EVM) and probability of error for different digital modulation schemes are presented briefly.

2.1 Receiver Front end

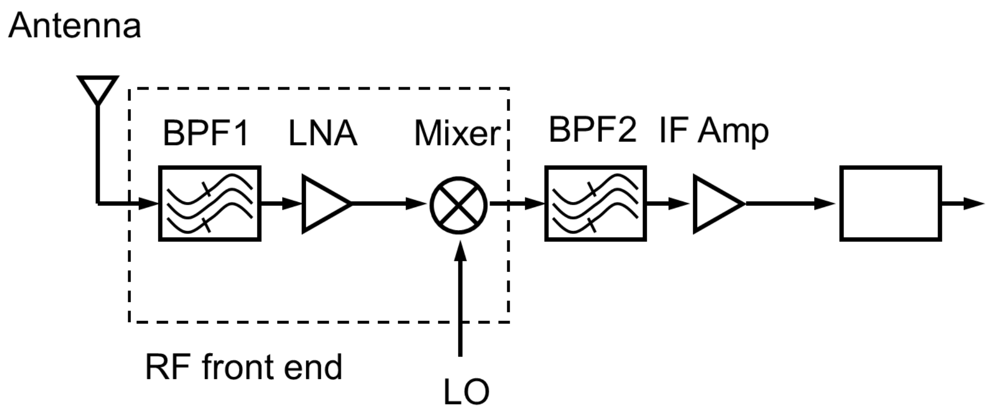

Figure (2.1) heterodyne receiver front end

The figure (2.1) illustrates the heterodyne architecture. The RF signal received at the input of antenna travels through the RF front end before demodulation. The RF front end has sub blocks that include LNA, mixers, and BPFs. Depending on the receiver architecture, the RF front end has various sub block arrangements. The purpose of RF front end is to perform amplification, frequency translation, channel selection, and interference mitigation.

2.2 Receiver Desensitization

Nonlinear properties of the receiver manifests when strong undesired signals present at the input of the receiver. This phenomena is called receiver desensitization. These large undesired signal degrades the sensitivity of the receiver. Receiver sensitivity is defined as minimum signal level required to interpret the received information. For digital communication systems, this is expressed in BER. Depending on the applications, the required SNR varies. For instance

DECT system [31] needs 25dB SNR at the input of the demodulator to maintain the quality of the signal.

2.2.1 Low noise amplifier

LNA is one of the key components in the receiver architecture. The function of LNA is to boost the weakest signal at the input of RF front end and reduce the noise contribution from subsequent stages. Since the noise figure of the receiver system is dominated by the first block [2], low noise amplifiers are designed to have high gain and low noise figure. Because increasing the gain of LNA improves the system noise figure.

The nonlinearities associated with LNA are gain compression, noise figure increase, intermodulation products and spurious responses.

2.2.2 Mixer

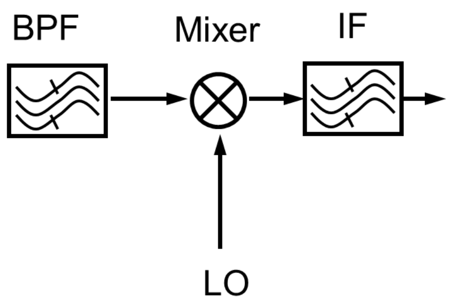

Figure (2.2) Mixer

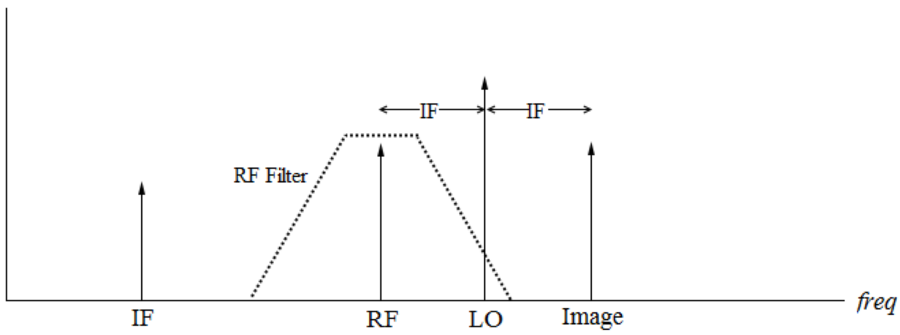

Figure (2.3) Mixer with low side injection

Mixer frequency translates by multiplying two signals. Mixer has two input ports for RF signal and LO signal. Depending on the LO signal frequency, the RF signal can be either down converted or up converted. The converted RF signal falls into IF frequency. In general, the receivers use down conversion. Frequency selective filters are used in front of the mixer to reject the image frequency that interferes with the desired signal. Since the incoming signal and noise are amplified by previous stage, mixers are required have high linearity and low noise figure.

The nonlinearities associated with mixers are gain compression, intermodulation products, and reciprocal mixing.

2.3 Behavioral modeling/Mathematical modeling

The behavioral modeling of RF blocks are based on standard system level specifications [10]. Therefore does not require detailed circuit specifications. For instance, system specification of specific RF block requires gain, noise figure, 1-dB compression point, IIP3, and bandwidth. These can be obtained from input output characteristics of the RF block. With these specifications, mathematical models can be developed to describe the nonlinearities of the particular block. The following sections describe nonlinearities of LNA and behavioral modeling for blocking and blocker noise figure.

2.3.1 Blocking

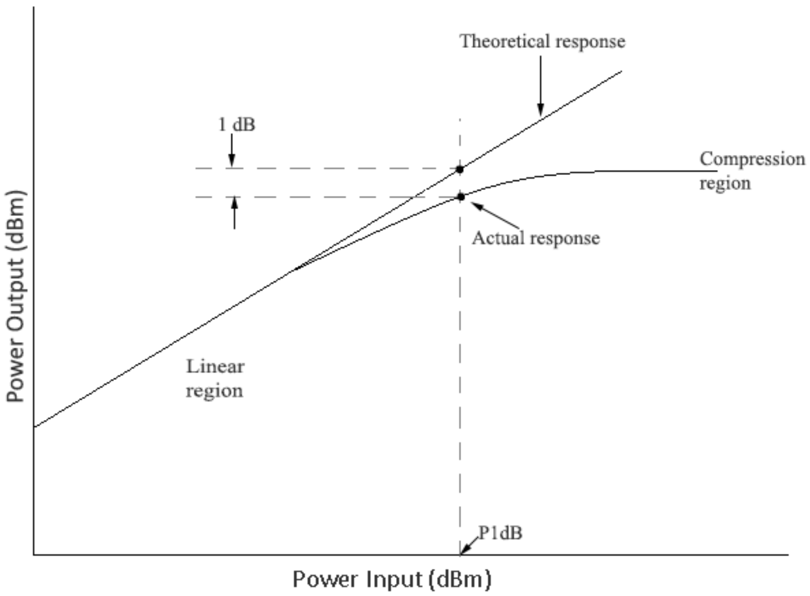

Figure (2.4) input output characteristics of a nonlinear device

When a strong interferer signal combined with weak desired signal is sent to a nonlinear component, strong signal tends to attenuate the small signal gain. Therefore, the desired signal experiences reducing gain with an increase in interferer power. At some instances, interferer is sufficiently large enough to cause the desired signal gain to drop to zero [1]. This type of desensitization is called blocking effect.

Figure (2.4) illustrates the input output characteristics of a theoretical response and practical response. In the linear region, both theoretical and practical curve has same response. Near the 1-dB compression point, the practical response starts to deviate from the theoretical response leading to saturation as the input power increases. 1-dB compression point is defined as the amount power needed to cause 1dB drop in the gain. And this response can be mathematically modeled using Taylor series expansion.

Assuming the incoming signal at the input of the LNA/Mixer has both desired signal and interferer, it can be expressed as below,

$$V_i = V_d \cos(\omega_d t) + V_b \cos(\omega_b t) \quad (1)$$

Where,

V_i: Incoming signal at the input of LNA/Mixer
V_d: Desired signal voltage
V_b: Blocker signal voltage
ω_d: Desired signal frequency
ω_b: Blocker frequency

Substituting equation (1) in Taylor expansion gives outgoing signal from the LNA/Mixer block.

$$V_o = \alpha_1 V_i + \alpha_2 V_i^2 + \alpha_3 V_i^3 + \cdots \quad (2)$$

And expanding the equation (2) gives infinite number of terms [9]. However first few terms are sufficient to model weakly nonlinear [2] gain compression behavior of the wanted signal and it is a function of desired signal frequency. This can be expressed as below,

$$V_o = \left(\alpha_1 - \frac{3}{2}\alpha_3 V_b^2\right) V_d \cos(\omega_d t) \quad (3)$$

Where,

α_1: Linear gain of LNA
α_3: Third order product

The negative sign before the second term of the equation (3) denotes compressive behavior of the nonlinear device. α_3 Is determined from the input 1-dB compression point blocker voltage and linear gain [2] and can be defined by (4).

$$\alpha_3 = \frac{0.0724 * \alpha_1}{V_{b-1db}^2} \quad (4)$$

Similarly α_3 can be defined for 3-dB blocking point.

$$\alpha_{3-3db} = \frac{0.195\alpha_1}{V_{b-3db}^2} \quad (5)$$

From equation (3), the small signal gain of the desired signal as a function of blocker voltage can be express as below,

$$G_{ssg} = \left(\alpha_1 - \frac{3}{2}\alpha_3 V_b^2\right) \cos(\omega_d t) \quad (6)$$

The Equation (6) is a good firsthand estimate for modeling the gain compression of weakly nonlinear device. However, if the device is strongly nonlinear, higher order terms should be included to describe the compressive behavior.

2.3.2 Noise factor modeling of LNA/Mixer

Another form of receiver desensitization is due to the noise factor increase of a single stage RF block in the presence of a strong blocker. It is assumed that increase in the noise factor is due to the nonlinearities that cause noise folding from the frequencies outside the bandwidth of interest. The mathematical model was developed for a single stage that describes the behavior of the NF increase as function of blocker power [3]. The equation is expressed as below,

$$F_{nl} = F_0\left(1 + \left(\frac{V_d}{V_{6-dB}}\right)^2\right) \quad (7)$$

Where,

F_{nl}: Noise factor of the nonlinear RF block
F_0: Small signal noise factor of the RF stage
V_d: Blocker voltage
V_{6-dB}: 6dB blocking level

Similarly equation (7) can be used to express the noise factor increase in the mixer stage as a function of the blocker assuming the local oscillator noise contribution is large enough to cause the increase in the mixer noise factor [3].

2.3.3 Intermodulation interference

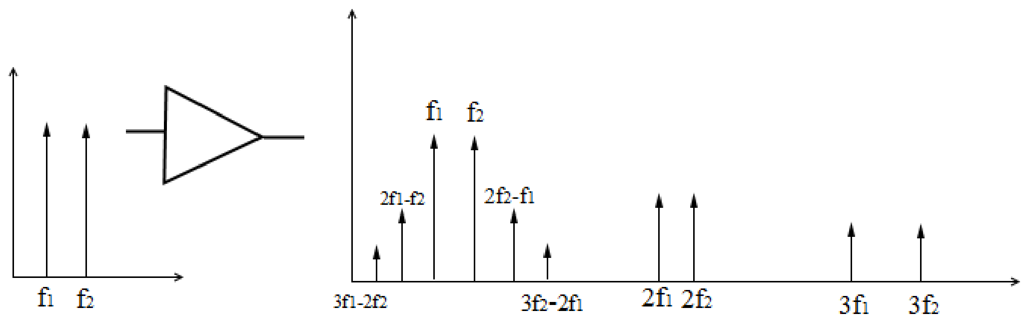

Figure (2.5) Intermodulation products

Intermodulation interference at the receiver is caused by either adjacent signals or strong out of band blockers loading the receiver front to produce undesired frequencies that fall under desired bandwidth, thus corrupting the desired signal [2]. Out of all intermodulation products, third order intermodulation products are of major concern, since they fall near the desired signal and has large amplitude compared to other intermodulation products. This significantly effects the performance of the receiver. These signals can be removed either filtering or active cancellation [4].

2.3.4 Harmonics and Spurious responses

Harmonics and spurious responses pose serious threat to the receiver performance. These distortions can be either created inside the receivers due to nonlinearity or received from the adjacent transmitters that fall under the passband of the receiver [4]. However, most of the cases these distortions can be avoided using bandpass filters.

2.3.5 Reciprocal mixing

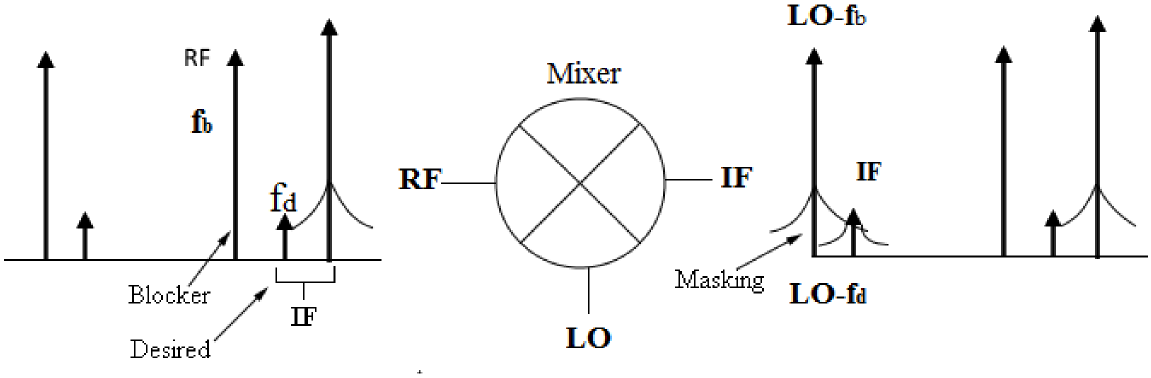

Figure (2.6) Reciprocal mixing

Reciprocal mixing is due to the phase noise of the LO signal mixing down into IF frequency point. In other words, the phase noise is random frequency fluctuations of the LO signal, that appear as noise sidebands on both side of the LO signal. This noise spectrum gets mixed down along with incoming RF signals. When a strong interferer along with a weak desired signal are at the input of the mixer, the down converted weak desired signal suffers from the masking of phase noise. And this would hinder the reception of the desired signal [9].

2.3.6 System modeling

System modeling is the complete receiver model that is developed using the MATLAB software incorporating the mathematical models, and modulation techniques to analyze the performance of the receiver when exposed to strong interferers. Baseband modeling was adapted since they reduce the execution time compared to passband model [10].The software developed model is based on the measurement setup.

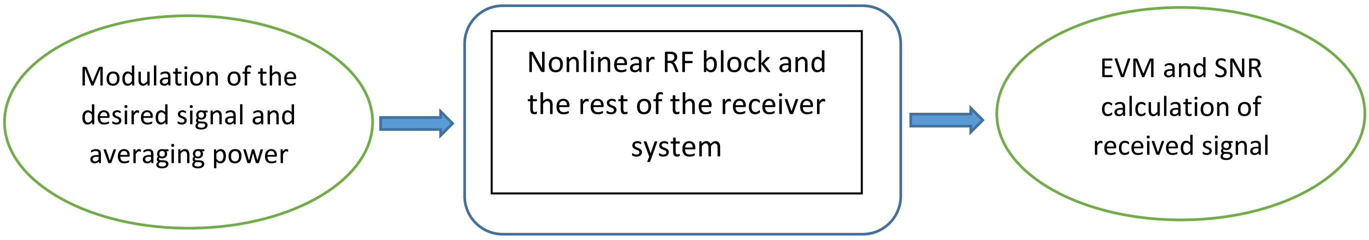

Figure (2.7) Stages of system modeling

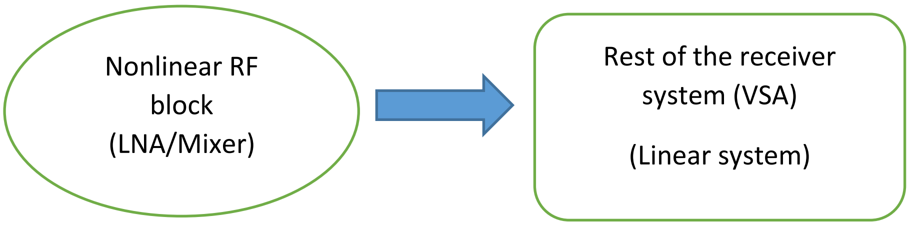

Figure (2.8) Cascaded noise figure stages

As seen in the figure (2.7), the system modeling consists series of stages. The first stage involves modulation of integer bits and averaging them to desired signal power level in dBm. The second stage includes nonlinear RF block incorporating the behavioral model described in the previous section and rest of the receiver system which is the VSA in this project, and third stage is EVM and SNR calculation of the received signal. The figure (2.8) illustrates the detailed second stage for system noise figure calculation. The friis formula [2] was used for calculating cascaded noise factor including the nonlinear noise factor model from the section 2.2.2. The cascaded noise factor can be defined by (7)

$$F_{tot} = F_{nl} + \frac{F_{sys}-1}{G_{ssg}} \quad (8)$$

Where,

F_{tot}: Total noise factor of the receiver
F_{sys}: Rest of the receiver system (VSA)

Further the cable and combiner losses were included in each stages as per the measurement.

2.4 Error vector magnitude

EVM is used as a performance metric in this project. Because it is very useful for multiple reasons. Firstly, it contains both amplitude error and phase error information that can be used to identify the type of distortion and the source of distortion of the system. Secondly, by normalizing the EVM, different modulation techniques can be compared directly against each other for a given average power level per symbol. Thirdly, EVM can be translated into SNR, and BER for different modulation techniques under assumption of AWGN channel performance [5].

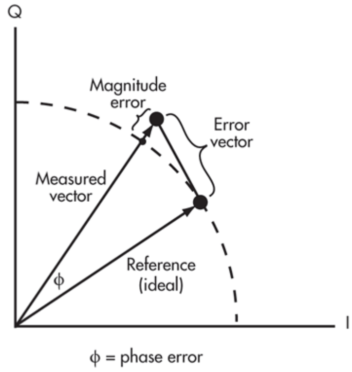

Figure (2.9) Error vector magnitude

RMS EVM is performed by summing the normalized received symbol points and the actual symbol points and dividing with average power of the total symbols transmitted [6].

Normalization factor can be written as,

$$A_{norm} = \sqrt{\frac{1}{P_v/T}} \tag{9}$$

Where,

P_v: Cumulative power of T symbols
T: Total number of symbols

The average power of the total symbols can be written as,

$$P_{avg} = \frac{1}{T}\sum_{p=1}^{T}[\sum_{q=1}^{T}\left(C_{i,ideal}^2 A_{norm}^2 + C_{q,ideal}^2 A_{norm}^2\right)] \tag{10}$$

Where,

$C_{i,ideal}$: In-phase ideal symbol point
$C_{q,ideal}$: Quadrature phase ideal symbol point

The RMS EVM of the can be represented as,

$$EVM_{RMS} = \sqrt{\frac{(\frac{1}{T})\sum_{r=1}^{T}\left((V_{i,meas}A_{norm} - C_{i,ideal}A_{norm})^2 + (V_{q,meas}A_{norm} - C_{q,ideal}A_{norm})^2\right)}{P_{avg}}} \tag{11}$$

Where,

$V_{i,ideal}$: In-phase measured symbol point
$V_{q,ideal}$: Quadrature phase measured symbol point

Normalization factor is calculated separately for measured symbols and ideal symbols.

The relationship between EVM and SNR can be defined by (12) [5],

$$EVM_{RMS} \approx \sqrt{\frac{1}{SNR}} \tag{12}$$

2.5 Probability of Error for various Digital modulation techniques

Digital modulation techniques	Probability of Error
BPSK	$P_b = Q\left(\sqrt{\frac{2E_b}{N_0}}\right)$
QPSK	$P_b = Q\left(\sqrt{\frac{2E_b}{N_0}}\right)$
M-QAM	$P_b = \frac{4}{log_2 M} Q\left\{\sqrt{\frac{3E_b log_2 M}{N_0(M-1)}}\right\}$

Table (2.1) Probability of Error for coherent digital modulation schemes

The table (2.1) provides the theoretical BER for different modulation schemes. These equations are used to compare the BER performance for different blocker powers.

Chapter 3

3. Experimental Setup

This chapter provides the reader with the description of the parameters, and experimental setups carried out during this project.

3.1 Hardware Specifications

The hardware specifications include the type of measurement equipment used, LNA, combiner

- **Signal generator:** Two signal generators were used for the experiments. The Agilent E4438C VSG for desired signal and Rhode & Schwarz SMS generator for CW blocker signal. Since different modulation techniques were used for comparing the BER performance, the Agilent VSG was used for generating modulated desired signal.
- **Vector signal analyzers:** The Agilent VSA N9020A MXA is an advanced tool for measuring and visualizing various signal parameters such as, channel power, ACPR, occupied bandwidth, intermodulation products, complex frequency spectrum, constellation diagrams for various modulation schemes, EVM, SNR and etc.
- **LNA**: The wideband low noise amplifier (RF Bay LNA-1440) is used in experiments. The datasheet can be found in [30].
- **Desired signal frequency:** The desired signal frequency was choose to be 394MHz. Since the focus is on receiver desensitization due to noise figure degradation, desired frequency was choose to be free of intermodulation and spurious products.
- **Bandpass filters**
- **Band reject filters**
- **Attenuators**
- **Combiner**

3.1 Measurements

This section deals with test setup for measuring small signal gain and noise figure of the LNA-1440 and mixer.

3.1.1 Characterization of LNA/Mixer

Characterization of LNA/Mixer involves single tone measurement of the DUT to find rudimentary parameters that can provide basic idea of the device performance. In the case of LNA/Mixer, linear gain and 1-dB compression point of single tone indicate amplification factor, the input power point where nonlinear behavior starts (see section 2.3).

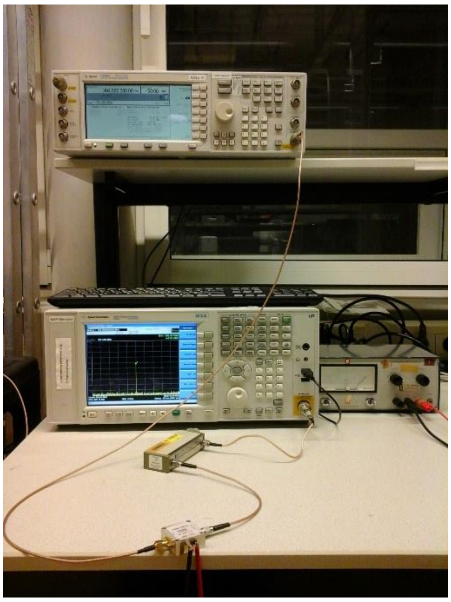

Figure (3.1) illustrates the test setup for single tone measurement

Figure (3.2) Single tone input output characteristics

The measurement setup consists of Agilent VSG, LNA-1440, tunable attenuator, DC blocker, and a VSA. The desired signal frequency was set to 394MHz. The desired signal power was swept from -80dBm till 5dBm in 1dB steps and the corresponding output power was measured in VSA spectrum analyzer mode. The measured output was plotted against input power compensating cable and attenuator losses. The HP attenuator and DC blocker were used at the input of VSA to avoid any potential damages to the VSA system.

3.1.2 Two tone measurement of LNA/Mixer

The procedure for two tone measurement is quite similar to the single tone measurement. In this case, the output power of the desired signal was measured as a function of interferer power. The desired signal power was maintained at -90dBm and interferer power was swept from -90dBm to 5dBm in 1dB steps. The measured desired output power was plotted against the interferer power to determine the gain and input 1-dB compression point. The measured and simulated results will be discussed in Chapter 4.

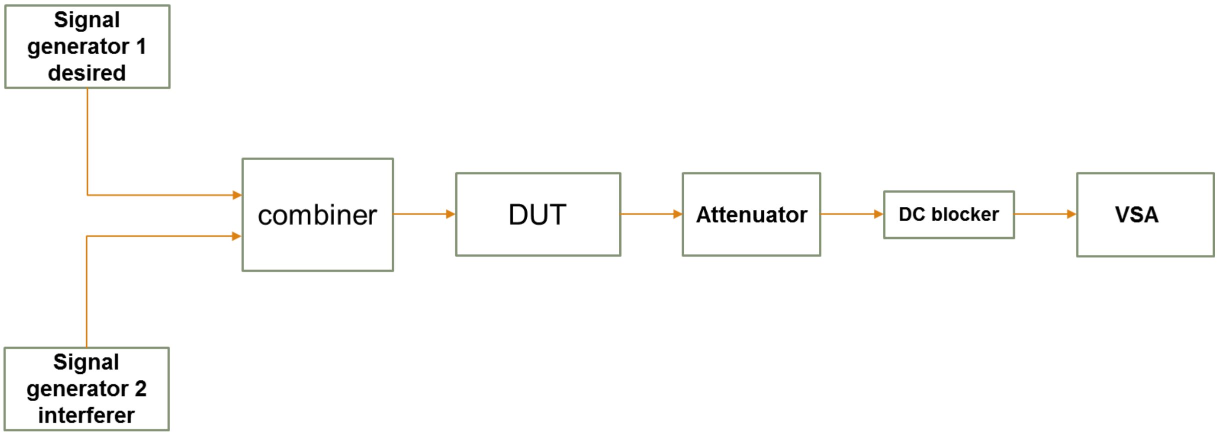

Figure (3.3) Block diagram of two tone measurement

The test setup consists of Agilent VSG for generating in band desired signal, Rhode & Schwarz SMS for generating OOB interferer, VSA, attenuator, combiner, and DC blocker. Few precautionary steps were followed to avoid any pitfalls while measuring. It is very important to isolate the generators because the improper isolation between the generators can result in reverse intermodulation products propagating through DUT and appearing at the output of VSA and reflections that affect the signals. To prevent this, 3-dB attenuators were placed on the output of the generators. And in general, two tone measurements are susceptible to various nonlinear behavior from different sources such as DUT, VSA, and coupling from antennas that adds with desired signal. Therefore, these possibilities should be considered during the measurement.

Further generators and VSA were synchronized with 10MHz reference clock signal for optimum performance. The attenuator and DC blocker used for the same reason mentioned in section 3.1.1.

3.1.3 Blocker noise figure measurement

The goal is to measure the noise figure increase in the DUT as function of interferer. The typical test setup for blocker noise figure can be seen in [9]. Which includes noise source, blocker generator, noise figure meter, isolator, filters, and DUT. Isolator is very crucial to this measurement because it protects the noise source from the blocker for accurate measurement. Due to the unavailability of isolator in the laboratory, different method was followed to determine the blocker noise figure. This method utilizes SNR measurement to determine the blocker noise figure.

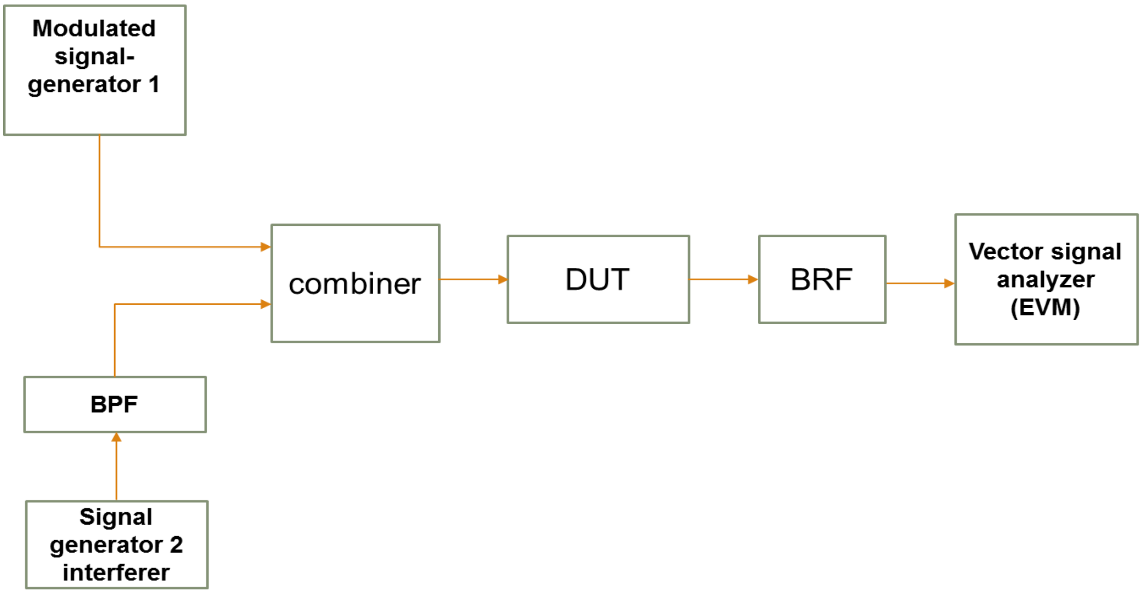

Figure (3.4) Block diagram of blocker noise figure

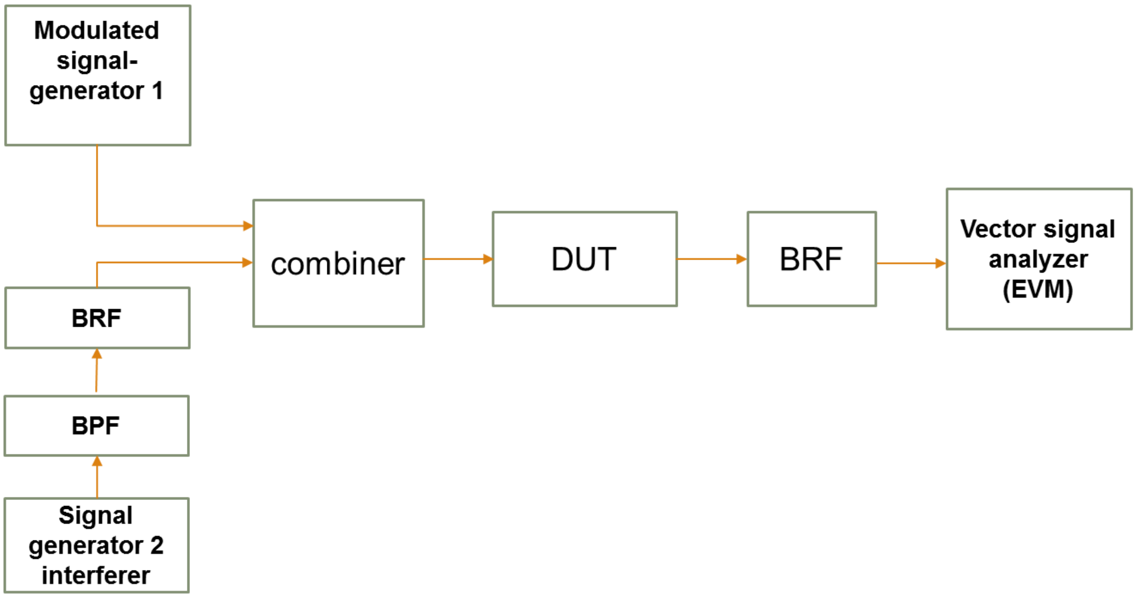

Figure (3.5) Non blocker setup

The test setup in figure (3.6) serves as reference to the test setup in figure (3.5). That is, when the blocker power is well within the linear range of the DUT, it shouldn't affect the SNR performance of the receiver system. Nevertheless, in the case of blocker noise figure setup, at higher blocker levels, DUT becomes nonlinear thus leading to SNR degradation of the system.

The notch filters were used at the output of the DUT in blocker noise figure setup to prevent from large blocker signal loading the internal mixer of the VSA. For this purpose, two notch filter with nearly 90dB rejection at blocker frequencies were used in the measurement setup. In addition to this, it is important to keep the desired signal within the linear range of the internal mixer to prevent the influence of mixer noise. The internal mixer specification of the

VSA can be found in [26]. The BPF was used after blocker generator to prevent noise from outside the blocker frequency to propagate inside the DUT.

The blocker noise figure calculation is explained in steps below,

1. The noise figure of the DUT was measured with the help of Agilent noise figure analyzer over the frequency range of the DUT. More information on measuring with noise figure analyzer can be found in [19].
2. The desired signal was QPSK modulated and set to -90dBm at 394MHz. The blocker was set at 410MHz and its power was swept from -90dBm to 5dBm in 1dB steps to measure the corresponding EVM of desired signal. From the measured EVM, $SNR_{out}$was calculated using the equation (12).
3. SNR_{in} At the input of the DUT was calculated assuming AWGN noise channel.
4. Subtracting SNR_{in} from SNR_{out} will give total noise figure of the system including DUT, VSA, and notch filters.

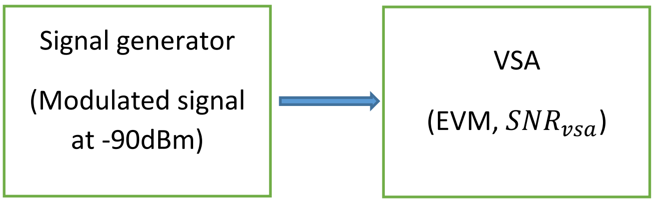

Figure (3.6) Noise figure of the VSA

5. To find the blocker noise figure of the DUT, the noise figure of the VSA and loss of notch filters should be known. The notch filter loss was neglected since they had less than 0.5dB insertion loss. The NF of the VSA system was found by directly connecting the generator to the VSA system to measure EVM. The calculation is shown below.
6. The blocker NF was calculated from substituting above variables in cascade NF equation mentioned in section 2.2.6.

Chapter 4

4. Results & Analysis

This chapter presents results and analysis of both simulation and measured data.

4.1 1-dB Compression point

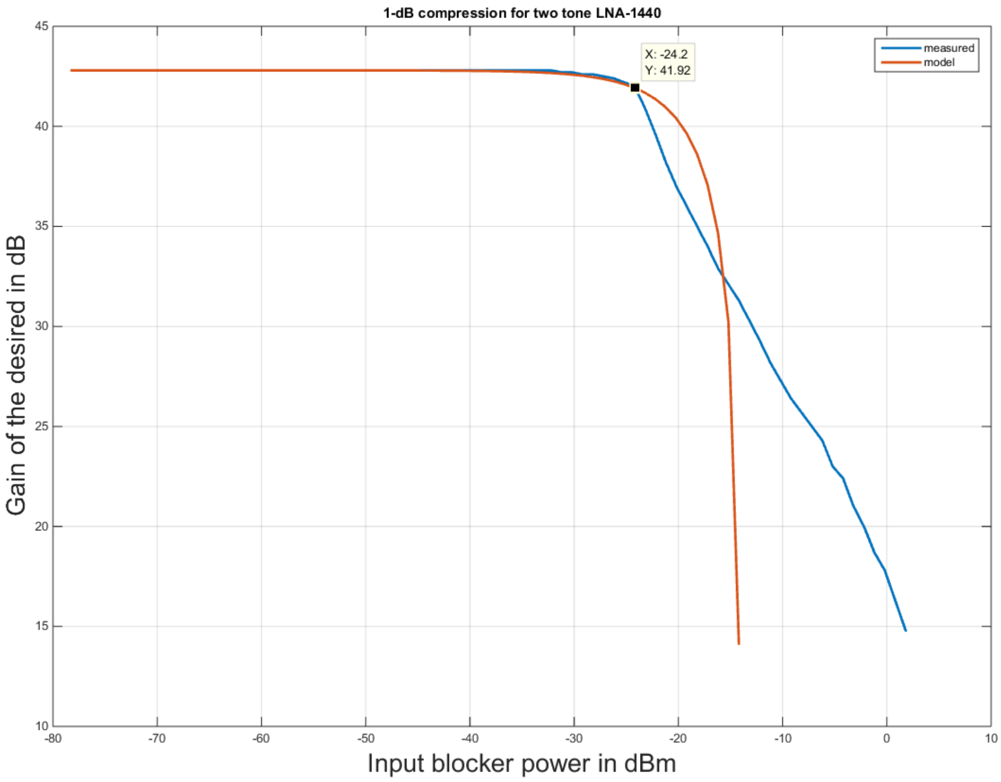

Figure (4.1) Small signal gain compression for measured and model

The measurement data of RF Bay LNA-1440 indicate small signal linear gain to be 42.8dB and input blocker level 1-dB compression point is at -23.7dBm.

Both measured curve and Taylor model are presented in the figure (4.1). Till 1-dB compression point (Blocker power is -24dBM), the model and the measured curve has good agreement. Signal region from -24 to -15dBm blocker power, the difference between measured curve and model has 3dB difference. Signal region from -15dBm to 0dBm, the gain of the measured curve decreases step by step fashion. However the gain the model decreases steeply. This is because, the Taylor model's nonlinear behavior defined only till cubic term [see equation (6)].

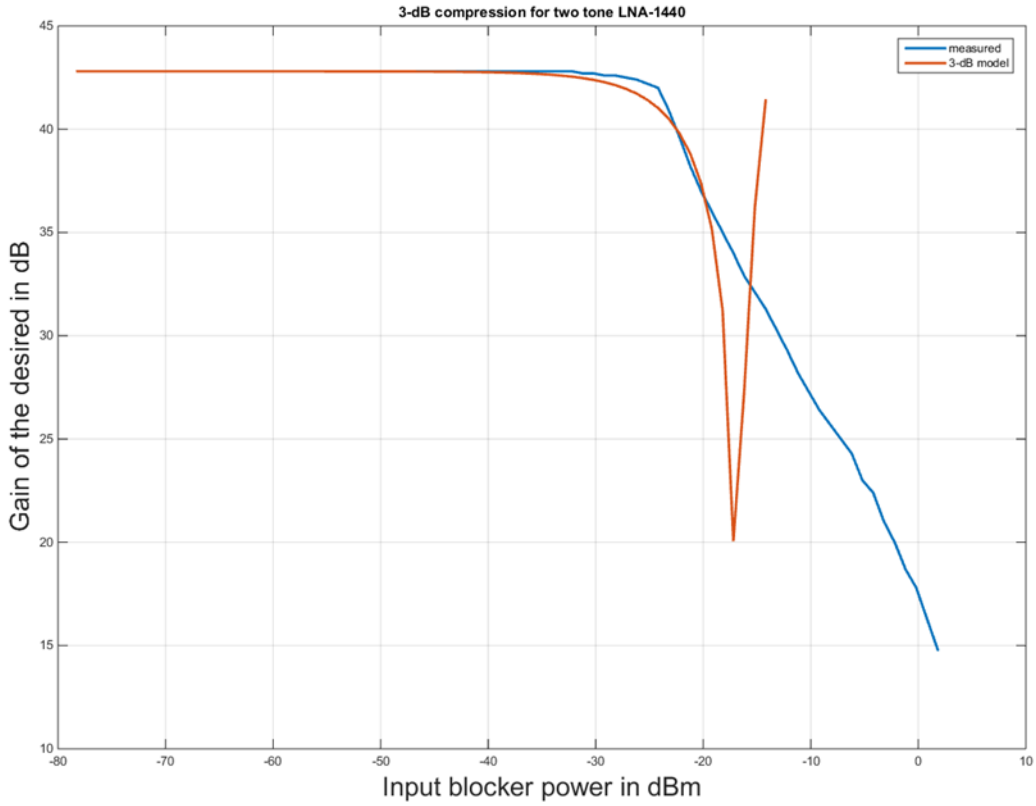

Figure (4.2) Small signal gain compression for measured and 3-dB model

In figure (4.2) the measured curve is compared against 3-dB blocking model [see equation (5)]. Signal power from -80dBm to -20dBm of blocker power, the Taylor model has good agreement with the measured curve. Further, in this region, the 3-dB model coincides with the measured curve at two instances. First instance is at 3-dB gain compression and second instance at 6-dB compression point. The difference between the measured and the model does not exceed more than 1dB. For blocker signal above -20dBm, the model becomes invalid.

In conclusion, 1-dB compression model represents best fit for describing nonlinear device till 1-dB gain compression point. Because, for any nonlinear device, input 1-dB compression point determines the maximum input power level for which device has linear response. And 3-dB blocking model, can be used till 6dB gain compression point. However, for large blocker levels (>-18dBm), higher order terms required to describe the behavior of the LNA.

4.2 Blocker noise figure

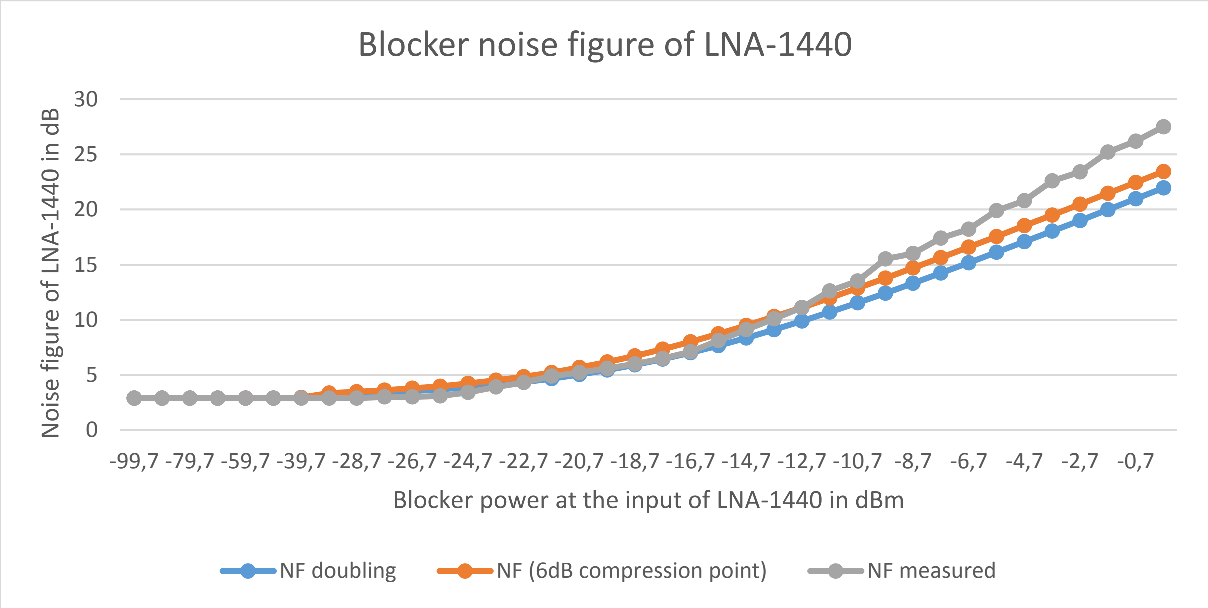

Figure (4.3) Blocker noise figure

The measured noise figure of LNA-1440 under no blocker conditions is 2.9dB.

The grey, blue, and orange curves represent measured blocker noise figure, noise figure model at noise factor doubling, and noise figure model at input 6dB compression blocker voltage point respectively. Signal level from -100dBm till -15dBm, both blocker noise figure models have good agreement with the measured data.

LNA-1440 Blocker power (dBm)	**Measured blocker noise figure (dB)**	**NF model for noise doubling blocker power (dB)**	**NF model for 6-dB compression input blocker power (dB)**
Input 1-dB compression blocker power (-23.7 dBm)	3.9	3.9	4
3dB compression blocker power (-21.7 dBm)	4.9	4.9	4.9
6dB compression blocker power (-19.7)	5.6	5.6	5.6

Table (4.1) Blocker noise figure comparison between the models and measured data

In summary,

- Blocker noise figure doubling requires, at least 6-dB gain compression from the LNA. This effect is due to, after 1-dB compression point, LNA becomes unstable producing spurious responses. These spurious responses cross modulates with noise spectrum outside the desired bandwidth to produce noise folding effect on the desired signal bandwidth.

- At higher blocker levels (>-10.7dBm), the difference between the model and the measured data is more than 3dB.

4.3 SNR

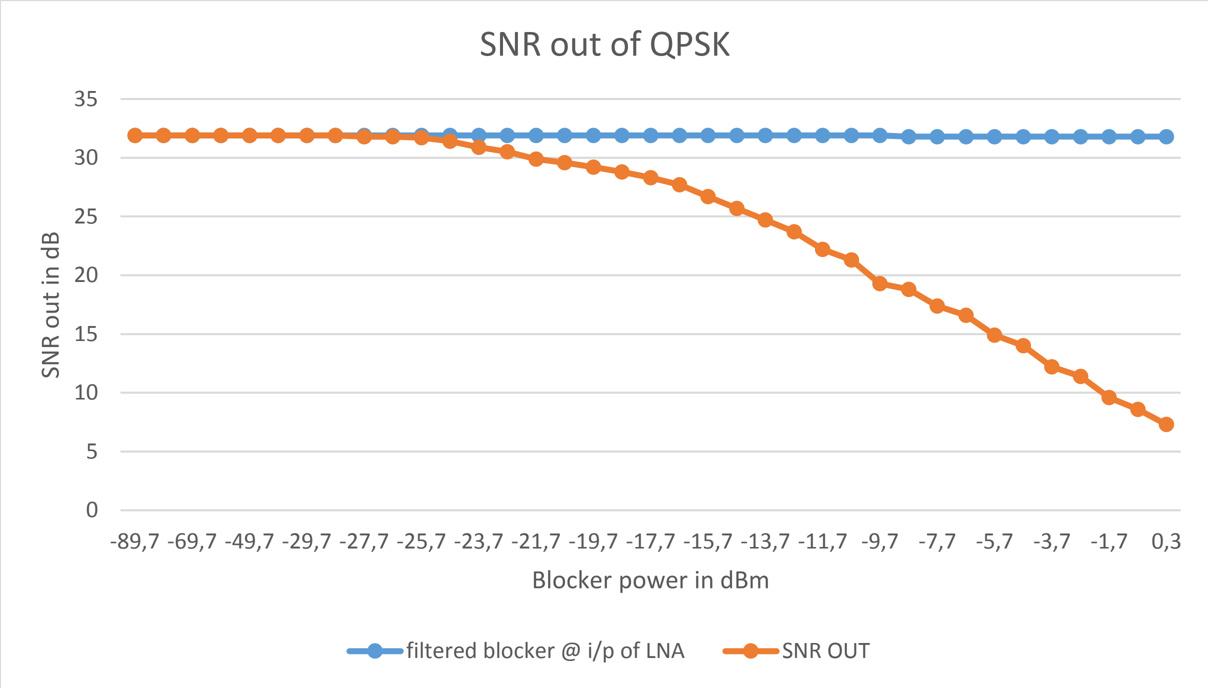

Figure (4.4) SNR comparison between no blocker and blocker scenario

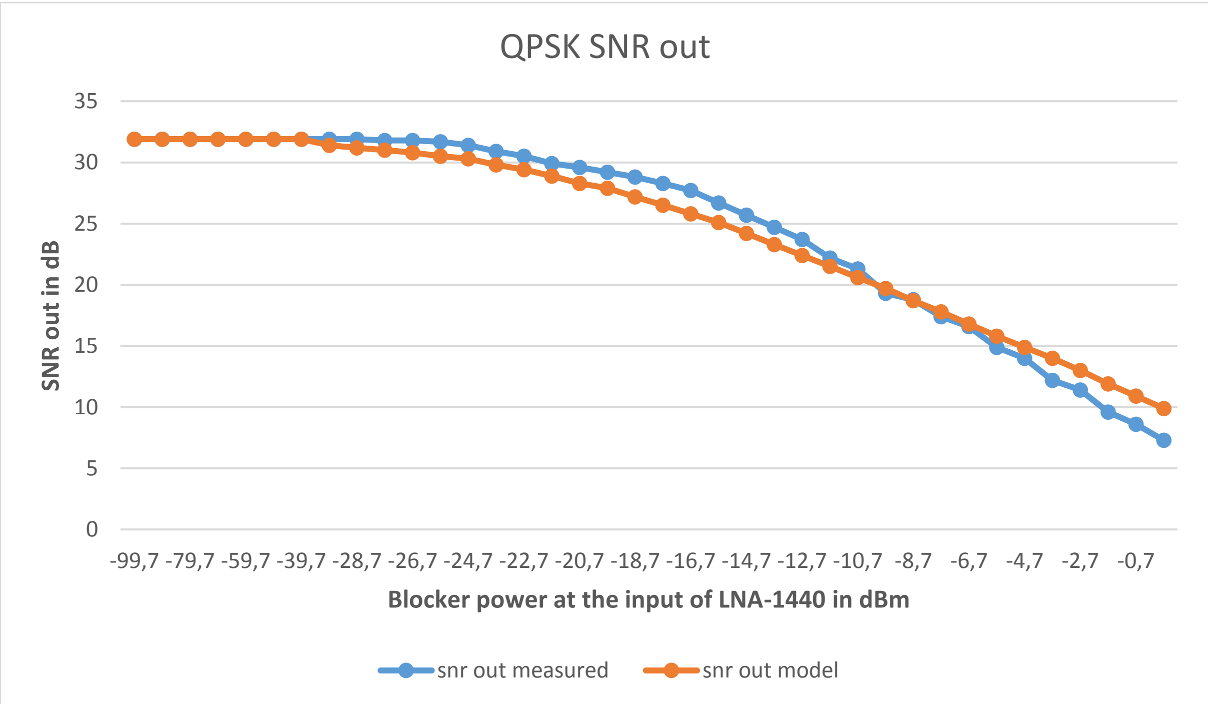

Figure (4.5) Signal to noise ratio of QPSK model and measurement data on LNA-1440

From the figure (4.5), it can be observed that the QPSK receiver model fits with measured results. For low blocker levels, the SNR does not change. At 3-dB compression point, the SNR drops from 32dB to 29.6dB. AT 6dB compression point, SNR drops by 3dB.

4.4 BER

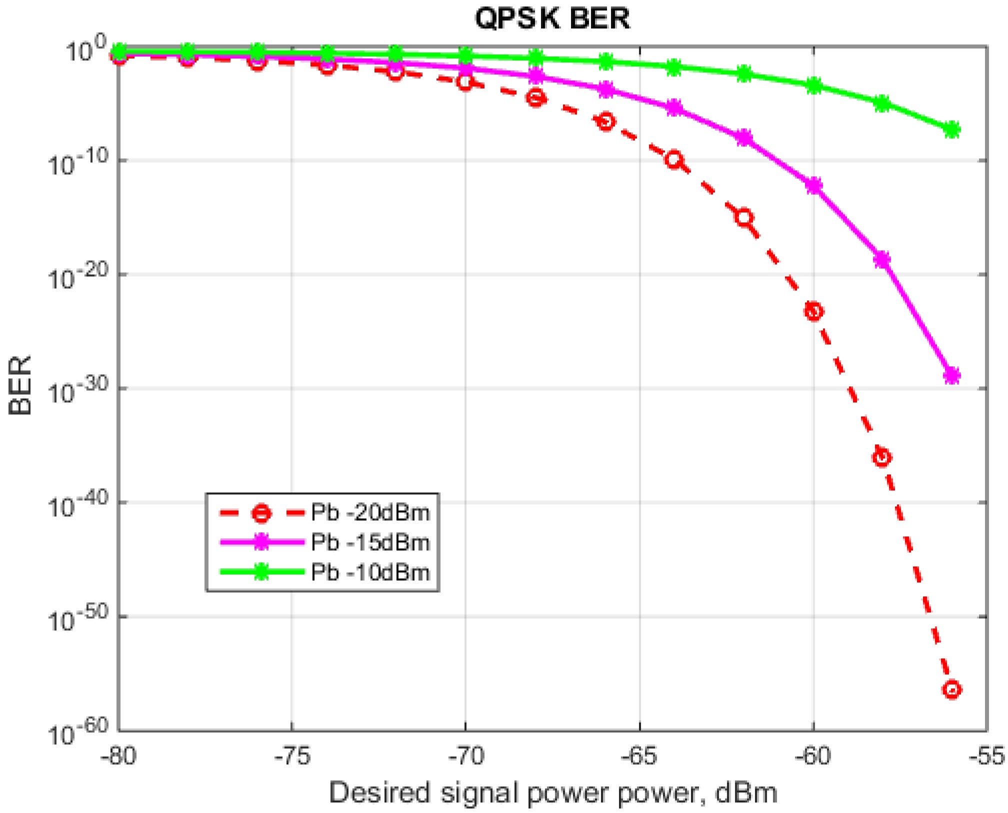

Figure (4.6) Desired power Vs BER for QPSK

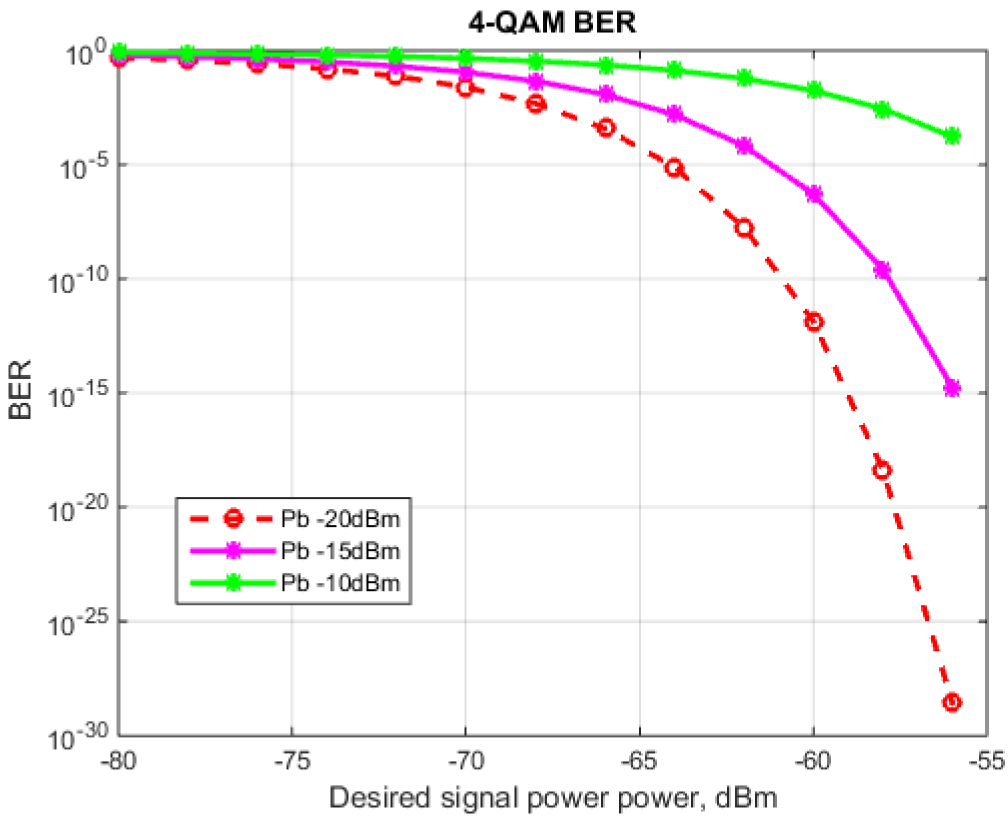

Figure (4.7) Desired power Vs BER for 4-QAM

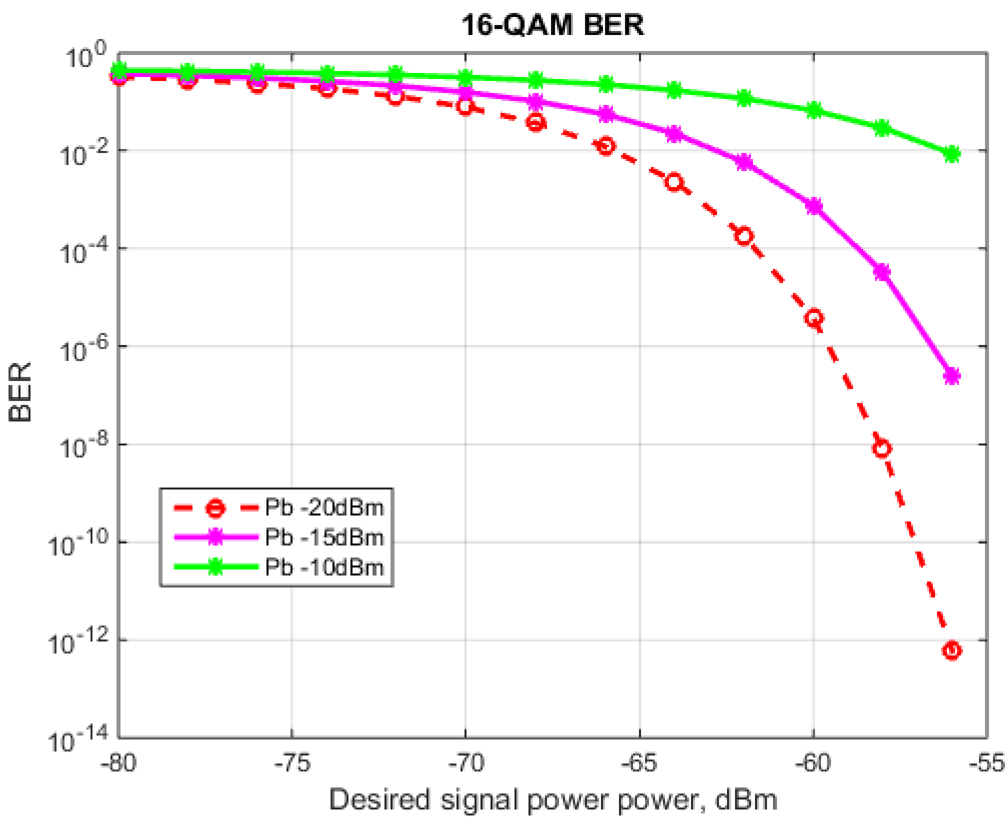

Figure (4.8) Desired power Vs BER for 16-QAM

The figures above compare the performance of the digital modulation schemes for different blocker power conditions. These BER graphs are based on blocker noise figure measurement.

In summary,

- For a given bitrate of the signal, QPSK has better performance over 4-QAM and 16-QAM for all blocker levels.
- For blocker power at -20dBm, to achieve BER of10^{-5}, the desired signal level should be above -70dBM, -65dBm, -62dBm for QPSK, 4-QAM, 16-QAM respectively. Similarly for blocker level at -10dBm, the desired signal level should be above -60dBm, -55dBm, -50dBm for QPSK, 4-QAM, 16-QAM respectively.
- In the worst case scenario, a weak signal (below -90dBm) entering the receiver needs more than 20dB amplification in order to maintain the quality of the signal.

Chapter 5

5. Conclusion

In this chapter, the conclusions for overall work that was carried during the master research project is presented by answering the research question.

The comparison between simulation and measurements on QPSK receiver indicate that the complete system model based on blocker noise figure and gain compression model show that the behavioral model agrees with measured data. The system modeling can be used to identify which block contributes to the SNR degradation at the output of the receiver. In this case, noise figure of LNA is contributes to the SNR degradation in the receiver. The noise contribution from the VSA was negligible due to the large gain of the LNA-1440.

Recommendations

Interference on radio receivers is a wide area of research. It includes modeling nonlinear properties of the receiver under various interference conditions, and effective interference mitigation techniques. This indicate interesting future research options, which are given below.

1. Behavioral modeling of blocker noise figure for mixers an incorporating them in system model.
2. Modeling nonlinear receiver properties under pulsed interference and wideband noise.
3. Interference mitigation techniques

Bibliography

[1] Stefan van de Beek, and Frank Leferink. "Robustness of a TETRA Base Station Receiver against Intentional EMI". IEEE transactions on electromagnetic compatibility.

[2] Behzad Razavi, RF Microelectronics, Second Edition.

[3] Flemming Hansen. "Desensitization in Transistorized PH/FM-Receivers". STORNO, Copenhagen, Denmark.

[4] Mark B. Bahu, Louis L.Taylor, "Tactical communication EMI/EMC co-site problems and solutions". 1994 IEEE.

[5] Rishad Ahmed Shafik, Md. Shahriar Rahman, and AHM Razibul Islam. "On the Extended Relationships Among EVM, BER and SNR as Performance Metrics". 4th International Conference on Electrical and Computer Engineering ICECE 2006, 19-21 December 2006, Dhaka, Bangladesh.

[6] Michael D. McKinley, Kate A. Remley, Maciej Myslinski, J. Stevenson Kenney, Dominique Schreurs, and Bart Nauwelaers. "EVM Calculation for Broadband Modulated Signals". 64^{th} ARFTG conf. Dig., FL, pp 45-52, Dec 2004.

[7] Jacques J. Gavan, and Meyer B. Shulman. "Effects of Densensitization on Mobile Radio System Performance, Part I: Qualitative Analysis". 1984 IEEE.

[8] Jacques J. Gavan, and Meyer B. Shulman. "Effects of Densensitization on Mobile Radio System Performance, Part II: Qualitative Analysis". 1984 IEEE.

[9] William Domino, Nooshin Vakilian, and Darioush Agahi. "Polynomial Model of Blocker Effects on LNA/Mixer Devices, An analysis of interference effects on small-signal gain and noise figure".

[10] Jesse E. Chen. "Modeling RF Systems".

[11] Dr. J. Gavan, and Elya B. Joffe. "High Power Broadcasting Skywave Transmitters Interference Analysis for navigation and Communication Systems". IEEE Transactions on Broadcasting, Vol. 36. No. I, March 1990.

[12] Yakup Bayram, John L. Volakis, Suk Keun Myoung, Seok Joo Doo, and Patrick Roblin. "High-Power EMI on RF Amplifier and Digital Modulation Schemes". IEEE transactions on electromagnetic compatibility, VOL. 50, NO. 4, November 2008.

[13] Stefan van de Beek, and Frank Leferink. University of Twente, Enschede, Thales Nederland B.V., Hengelo. "Current Intentional EMI studies in Europe with a Focus on Structures". 2014 IEICE.

[14] Ray R. Tanuhardja, Stefan van de Beek, Mark J. Bentum, and Frank B. J. Leferink. "Vulnerability of Terrestrial-Trunked Radio to Intelligent Intentional Electromagnetic Interference". IEEE transactions on electromagnetic compatibility.

[15] F.H.Sanders, R.L.Hinkle, and B.J.Ramsey. "Analysis of Electromagnetic Compatibility between Radar Stations and 4 Ghz Fixed-Satellite Earth Stations". U.S.Department of Commerce, July 1994

[16] Stefan van de Beek, Robert Vogt-Ardatjew, and Frank Leferink. "Intentional Electromagnetic Interference through Saturation of the RF Front End". APEMC 2015.

[17] Prof. Ali M. Niknejad. "Integrated circuits for communication".

[18] User's Guide. "Agilent Technologies ESG Vector Signal Generator".

[19] Application Note. "Agilent. Fundamentals of RF and Microwave Noise Figure Measurements".

[20] Product Note. "Agilent PN 89400-14. Using Error Vector Magnitude Measurements to Analyze and Troubleshoot Vector-Modulated Signals".

[21] Maoliu Lin, Qijun Zhang, and Qinghua Xu. "EVM Simulation and its Comparison with BER for Different Types of Modulation". 2007 IEEE.

[22] "Steps to a Perfect Digital Demodulation Measurement. Agilent PN 89400-14A".

[23] Product Note. "Agilent PN 89400-8. Using Vector Modulation Analysis in the Integration, Troubleshooting, and Design of Digital RF Communications Systems".

[24]" N9020A/N9010A Spectrum Analyzer Mode Measurement Guide". Agilent X-Series Signal Analyzer.

[25] Bob Muro. "Noise Terminology: An Overview of Noise Terminology and Applications".

[26] Whitham D. Reeve. "Noise Tutorial Part VI ~ Noise Measurements with a Spectrum Analyzer."

[27] Robert J. Achatz, Roger A. Dalke, and John J. Lemmon. "In-Building Radio Enhancement Systems for Public Safety". U.S. Department Of Commerce. September 2011.

[28] F.H.Sanders, R.L.Hinkle, and B.J.Ramsey. "Analysis of Electromagnetic Compatibility between Radar Stations and 4 Ghz Fixed-Satellite Earth Stations". U.S.Department of Commerce, July 1994.

[29] Edward Savage and William Radasky. "Overview of the Threat of IEMI (Intentional Electromagnetic Interference)". 2012 IEEE.

[30] RF Bay, Inc. LNA-1440. Retrieved from http://rfbayinc.com/products_pdf/product_88.pdf

[31] Bosco Leung, VLSI for wireless communication, Second Edition.

Appendix A: Measurement data

The measurement data for LNA-1440 is attached here.

Settings

desired freq	394MHz	
blocker freq	410MHz	
desired power	-70dBm	
RBW	10kHz	
VBW	10kHz	
span	50MHz	
MXA atten	10dB	
avg/hold		20

observed blocker frequency at MXA	410MHz
observed desired frequency at MXA	394MHZ
correction at LNA i/p blocker (verified)	-8,2dB
correction at LNA i/p desired	-8,3dB
physical attenuator loss	31,6dB

LNA-1440 two tone 1-dB compression point measurement						
Blocker power in dBm	actual blocker power at LNA i/p	MXA desired ouput in dBm	MXA output corrected for attenuator	Pd at the LNA i/p	gain of desired	power gain
-70	-78,2	-67,1	-35,5	-78,3	42,8	19054,60718
-65	-73,2	-67,1	-35,5	-78,3	42,8	19054,60718
-60	-68,2	-67,1	-35,5	-78,3	42,8	19054,60718
-55	-63,2	-67,1	-35,5	-78,3	42,8	19054,60718
-50	-58,2	-67,1	-35,5	-78,3	42,8	19054,60718
-45	-53,2	-67,1	-35,5	-78,3	42,8	19054,60718
-40	-48,2	-67,1	-35,5	-78,3	42,8	19054,60718
-39	-47,2	-67,1	-35,5	-78,3	42,8	19054,60718
-38	-46,2	-67,1	-35,5	-78,3	42,8	19054,60718
-37	-45,2	-67,1	-35,5	-78,3	42,8	19054,60718
-36	-44,2	-67,1	-35,5	-78,3	42,8	19054,60718
-35	-43,2	-67,1	-35,5	-78,3	42,8	19054,60718
-34	-42,2	-67,1	-35,5	-78,3	42,8	19054,60718
-33	-41,2	-67,1	-35,5	-78,3	42,8	19054,60718
-32	-40,2	-67,1	-35,5	-78,3	42,8	19054,60718
-31	-39,2	-67,1	-35,5	-78,3	42,8	19054,60718
-30	-38,2	-67,1	-35,5	-78,3	42,8	19054,60718
-29	-37,2	-67,1	-35,5	-78,3	42,8	19054,60718
-28	-36,2	-67,1	-35,5	-78,3	42,8	19054,60718
-27	-35,2	-67,1	-35,5	-78,3	42,8	19054,60718
-26	-34,2	-67,1	-35,5	-78,3	42,8	19054,60718
-25	-33,2	-67,1	-35,5	-78,3	42,8	19054,60718
-24	-32,2	-67,1	-35,5	-78,3	42,8	19054,60718
-23	-31,2	-67,2	-35,6	-78,3	42,7	18620,87137
-22	-30,2	-67,2	-35,6	-78,3	42,7	18620,87137
-21	-29,2	-67,3	-35,7	-78,3	42,6	18197,00859
-20	-28,2	-67,3	-35,7	-78,3	42,6	18197,00859
-19	-27,2	-67,4	-35,8	-78,3	42,5	17782,7941
-18	-26,2	-67,5	-35,9	-78,3	42,4	17378,00829
-17	-25,2	-67,7	-36,1	-78,3	42,2	16595,86907
-16	-24,2	-67,9	-36,3	-78,3	42	15848,93192
-15	-23,2	-69	-37,4	-78,3	40,9	12302,68771
-14	-22,2	-70,3	-38,7	-78,3	39,6	9120,108394
-13	-21,2	-71,7	-40,1	-78,3	38,2	6606,93448
-12	-20,2	-72,9	-41,3	-78,3	37	5011,872336
-11	-19,2	-73,9	-42,3	-78,3	36	3981,071706
-10	-18,2	-74,9	-43,3	-78,3	35	3162,27766
-9	-17,2	-75,9	-44,3	-78,3	34	2511,886432
-8	-16,2	-77	-45,4	-78,3	32,9	1949,8446
-7	-15,2	-77,8	-46,2	-78,3	32,1	1621,810097
-6	-14,2	-78,6	-47	-78,3	31,3	1348,962883
-5	-13,2	-79,6	-48	-78,3	30,3	1071,519305
-4	-12,2	-80,6	-49	-78,3	29,3	851,1380382
-3	-11,2	-81,7	-50,1	-78,3	28,2	660,693448
-2	-10,2	-82,6	-51	-78,3	27,3	537,0317964
-1	-9,2	-83,5	-51,9	-78,3	26,4	436,5158322
0	-8,2	-84,2	-52,6	-78,3	25,7	371,5352291
1	-7,2	-84,9	-53,3	-78,3	25	316,227766
2	-6,2	-85,6	-54	-78,3	24,3	269,1534804
3	-5,2	-86,9	-55,3	-78,3	23	199,5262315
4	-4,2	-87,5	-55,9	-78,3	22,4	173,7800829
5	-3,2	-88,9	-57,3	-78,3	21	125,8925412
6	-2,2	-89,9	-58,3	-78,3	20	100
7	-1,2	-91,2	-59,6	-78,3	18,7	74,13102413
8	-0,2	-92,1	-60,5	-78,3	17,8	60,25595861
9	0,8	-93,6	-62	-78,3	16,3	42,65795188
10	1,8	-95,1	-63,5	-78,3	14,8	30,1995172

Blocker Noise figure

Noise figure measurement on LNA-1440					
Blocker	**actual Pb**	**SNR out without blocker**	**SNR out with blocker**	**SNR IN calculated**	**NOISE FIGURE OF LNA**
-90	**-99,7**	**31,9**	31,9	34,8	2,9
-80	-89,7	31,9	31,9	34,8	2,9
-70	-79,7	31,9	31,9	34,8	2,9
-60	-69,7	31,9	31,9	34,8	2,9
-50	-59,7	31,9	31,9	34,8	2,9
-40	-49,7	31,9	31,9	34,8	2,9
-30	-39,7	31,9	31,9	34,8	2,9
-20	-29,7	31,9	31,9	34,8	2,9
-19	-28,7	31,9	31,9	34,8	2,9
-18	-27,7	31,9	31,8	34,8	3
-17	-26,7	31,9	31,8	34,8	3
-16	-25,7	31,9	31,7	34,8	3,1
-15	-24,7	31,9	31,4	34,8	3,4
-14	-23,7	31,9	30,9	34,8	3,9
-13	-22,7	31,9	30,5	34,8	4,3
-12	-21,7	31,9	29,9	34,8	4,9
-11	-20,7	31,9	29,6	34,8	5,2
-10	-19,7	31,9	29,2	34,8	5,6
-9	-18,7	31,9	28,8	34,8	6
-8	-17,7	31,9	28,3	34,8	6,5
-7	-16,7	31,9	27,7	34,8	7,1
-6	-15,7	31,9	26,7	34,8	8,1
-5	-14,7	31,9	25,7	34,8	9,1
-4	-13,7	31,9	24,7	34,8	10,1
-3	-12,7	31,9	23,7	34,8	11,1
-2	-11,7	31,9	22,2	34,8	12,6
-1	-10,7	31,9	21,3	34,8	13,5
0	-9,7	31,9	19,3	34,8	15,5
1	-8,7	31,8	18,8	34,8	16
2	-7,7	31,8	17,4	34,8	17,4
3	-6,7	31,8	16,6	34,8	18,2
4	-5,7	31,8	14,9	34,8	19,9
5	-4,7	31,8	14	34,8	20,8
6	-3,7	31,8	12,2	34,8	22,6
7	-2,7	31,8	11,4	34,8	23,4
8	-1,7	31,8	9,6	34,8	25,2
9	-0,7	31,8	8,6	34,8	26,2
10	0,3	31,8	7,3	34,8	27,5